JOURNAL

OF THE AMERICAN CHEMICAL SOCIETY

VOLUME 110, NUMBER 2 JANUARY 20, 1988

High-Resolution ESR Spectroscopy and Structure of the Acetaldehyde Radical Cation (CH_3CHO^+) in Neon Matrices at 4 K: Comparison with Results in Freon Matrices

Lon B. Knight, Jr.,*† B. W. Gregory,† S. T. Cobranchi,† Ffrancon Williams,*‡ and Xue-Zhi Qin‡

Contribution from the Chemistry Department, Furman University, Greenville, South Carolina 29613, and University of Tennessee, Knoxville, Tennessee 37996.
Received March 16, 1987

Abstract: Detailed ESR studies are reported for the acetaldehyde radical cation (CH_3CHO^+) trapped in neon matrices. The cation was generated by photoionization, electron bombardment, or laser multiphoton ionization of dilute acetaldehyde neon mixtures (10^2 to 10^4 dilution factor) during codeposition on a flat target at 4 K. Its ESR spectrum was well resolved and showed strong preferential orientation effects, two sets of strong features being observed for field directions in the target plane, while another set of weaker line components became strongly enhanced when the field was applied normal to this plane. These results indicate that the cations are aligned with their CCHO planes parallel to the deposition surface. Accordingly, the largest principal value of the **g** tensor is found to be perpendicular to the CCHO plane, as previously determined for the formaldehyde cation (H_2CO^+). The measured values of the **g** and aldehydic ^1H hyperfine tensors are consistent with the assignment of the unpaired electron to the nonbonding oxygen-centered 10a′ molecular orbital which is, however, about 50% delocalized onto the aldehydic hydrogen (1s) and methyl carbon (2p) orbitals. The **g** and aldehydic ^1H **A** tensor components are the following: $g_x = 2.0069$ (3), $A_x = 355$ (1) MHz; $g_z = 2.0019$ (6), $A_z = 374$ (3) MHz, $g_y = 2.0026$ (3), $A_y = 353$ (1) MHz. The much smaller hyperfine interaction (4.3 MHz) with the hydrogens of the methyl group is exceedingly well resolved into a 1:1:1:1 quartet at 4 K with the field normal to the CCHO plane, and these intensity ratios indicate some form of restricted rotation of the methyl group, possibly via tunneling. In contrast to the neon studies, the ESR spectra of the acetaldehyde radical cation in Freon matrices show much poorer resolution and are complicated by the appearance of a highly structured anisotropic ^{35}Cl hyperfine interaction below 120 K. As expected for the formation of a σ^* complex between the in-plane oxygen 2p orbital from the SOMO of CH_3CHO^+ and a filled chlorine 3p orbital from a solvent ($CFCl_3$) ligand, the largest ^{35}Cl coupling is associated with the smallest g component along the σ^* bond direction. Despite this chlorine interaction, the average or isotropic aldehydic ^1H hf. coupling appears to be about 5–10% *larger* in $CFCl_3$ than in neon, indicating that spin delocalization to this β hydrogen in CH_3CHO^+ is remarkably insensitive to σ^* complex formation.

Recent years have witnessed considerable progress in the structural characterization of a wide range of radical cations by solid-state ESR spectroscopy.[1-3] This broad advance was initiated by the development of two quite distinct methodologies for the generation and trapping of these species under matrix isolation conditions. In the technique utilized by Knight and his group,[1] the cations are typically formed by photoionization or 50-eV electron beam irradiation during the codeposition of the sample vapor and the neon matrix gas on a target surface cooled by liquid helium to 5 ± 1 K. The photoionization method employs 16.8-eV photons from an open-tube neon resonance lamp so this technique of ion generation is very similar to that used in helium I photoelectron spectroscopy,[4] the important point being that a gas-like radical cation is generated either in the gas phase or, because of the low-energy radiation involved, at points extremely close to the trapping surface during the codeposition. A counteranion is also produced and trapped by this process in a matrix site well separated from the cation species.[5] Moreover, the chemical inertness of the matrix preserves the character of the gas-phase ion, as illustrated by the similarity between the ^{13}C hyperfine coupling determined for CO^+ in a neon matrix[6] and the value determined for this cation in the gas phase by microwave spectroscopy.[7]

The other approach which has been widely used for the generation of cations in the solid state[2,3] is based upon an adaptation of chemical reactions induced by high-energy radiation. A con-

† Furman University.
‡ University of Tennessee.

(1) Knight, L. B., Jr. *Acc. Chem. Res.* **1986**, *19*, 313.
(2) Shida, T.; Haselbach, E.; Bally, T. *Acc. Chem. Res.* **1984**, *17*, 180.
(3) Symons, M. C. R. *Chem. Soc. Rev.* **1984**, *13*, 412.
(4) Kimura, K.; Katsumata, S.; Achiba, Y.; Yamazaki, T.; Iwata, S. *Handbook of HeI Photoelectron Spectra of Fundamental Organic Molecules*; Halsted Press: New York, 1981; p 145.
(5) Knight, L. B., Jr.; Earl, E.; Ligon, A. R.; Cobranchi, D. P. *J. Chem. Phys.* **1986**, *85*, 1228.
(6) Knight, L. B., Jr.; Steadman, J. *J. Chem. Phys.* **1982**, *77*, 1750; *J. Am. Chem. Soc.* **1984**, *106*, 900.
(7) Piltch, N. D.; Szanto, P. G.; Anderson, T. G.; Gudeman, C. S.; Dixon, T. A.; Woods, R. G. *J. Chem. Phys.* **1982**, *76*, 3385.

0002-7863/88/1510-0327$01.50/0

venient source of such radiation consists of X- or γ-rays in the 200-keV–2-MeV range which can penetrate a bulk sample and produce a dispersion of Compton recoil electrons throughout the material. These fast electrons, whose initial energies lie within an order of magnitude of that possessed by the incident photon, mediate the transfer of energy to the absorber molecules by producing well-defined tracks made up of secondary ionization events. Although cations are readily produced in this way, it must be stressed that the simple expedient of incorporating an electron scavenger in the absorber at low concentration to prevent electron return to the cation does not, in general, lead to a viable irradiation method of producing these species for spectroscopic studies in solids,[8] the reason being that many radical cations are extremely reactive in ion–molecule reactions with their parent molecules.

Consequently, a generally suitable bulk irradiation method must allow the radical cation to be generated from a *dilute* solution of the parent molecule in a chemically inert environment. If the solute cations were only generated by direct electron impact, however, this stringent requirement would greatly lower the efficiency of the process, since the (e^-, $2e^-$) ionization process does not discriminate between solvent and solute molecules. Fortunately, this problem is nicely circumvented if the solute cations can be produced indirectly by positive charge transfer from the solvent cations, a process driven by an ionization potential difference between solvent and solute, and this turns out to occur when certain Freons are used as solvents.[2,9] In fact, Freon matrices are ideally suited for this technique since, in addition to having high ionization potentials, they also satisfy the requirements (a) of chemical inertness and (b) of electron attachment[10] to prevent return.

Thus, these two methods of cation generation for matrix ESR studies not only make use of different radiation energies, trapping techniques, and inert matrices, but they also differ with respect to the fundamental ionization mechanism that is employed. Moreover, the cations previously studied by these techniques fall into two exclusive groups, Knight's work describing small cations[1] such as AlF^+, SiO^+, N_2^+, CH_4^+, H_2O^+, and H_2CO^+, whereas the practitioners of the Freon method have concentrated on cations produced from larger organic molecules.[2,3] Indeed, this apparent dichotomy has been reinforced by reports of unsuccessful attempts to prepare CH_4^+ and H_2CO^+ by the Freon technique.[3,11] Nonetheless, while recognizing that in normal practice the two techniques may have rather separate areas of applicability and thereby to some extent complement each other, it seemed to be highly desirable to find a radical cation that could be studied in detail by both techniques so that the results could be compared. In this report we describe the first such comparative study of these two different matrix ESR methods for the specific case of the acetaldehyde radical cation.

There are three main reasons why the acetaldehyde radical cation was selected for this combined study. First, Knight and Steadman[11] have made a thorough ESR investigation of the prototype formaldehyde cation in a neon matrix, both the **g** and nuclear (^1H and ^{13}C) hyperfine tensors being fully characterized as a result of the excellent spectral resolution that was obtained. An important finding of this work[11] is that the largest component of the **g** tensor lies along a direction perpendicular to the radical plane rather than along the C_2 symmetry axis, although the latter assignment had been supposed in the analysis of poorly resolved patterns for the isoelectronic radicals H_2CN,[12] H_2BO,[13] and $H_2C_2^-$.[14] Thus, the ESR parameters for H_2CO^+ can provide benchmarks for the spectral interpretation of isostructural species and the more complex acetaldehyde radical cation.

Secondly, the ESR spectrum of CH_3CHO^+ in Freon matrices at 50–90 K is unusual in that the expected doublet features arising from the large coupling to the aldehydic hydrogen[11] show a complex substructure. This substructure was at first assigned to hyperfine coupling with the hydrogens of the methyl group,[15] but subsequent studies on the deuterated cations CD_3CHO^+ and CH_3CDO^+ showed this interpretation to be incorrect and that the interaction results mainly from a highly anisotropic coupling to a single chlorine nucleus in the $CFCl_3$ matrix.[16] Additional studies[17-19] have confirmed this conclusion, and the chlorine interaction is presumed to arise from a weak σ^* complex formed between the acetaldehyde radical cation and the $CFCl_3$ matrix.[16-19] This kind of matrix interaction should be minimized in a neon matrix because its ionization potential (21.6 eV) is much higher than that of acetaldehyde (10.26 eV),[4] and therefore it was of obvious interest to compare the complexed form of the cation in $CFCl_3$ with what should be a more pristine form in neon. Finally, the complexity of the low-temperature ESR spectrum of the acetaldehyde cation in $CFCl_3$ precludes a detailed analysis in terms of the **g** and ^1H hyperfine tensors. Quite independent of the degree of interaction between the radical cation and the matrix, this information should be more easily obtainable from ESR studies in a neon matrix given that the natural abundance of magnetic neon isotopes is extremely small.

Experimental Section

Neon Matrices. The trapping of the acetaldehyde radical cation in neon matrices was conducted at Furman University with the ESR matrix apparatus described in previous reports.[6,20] An Air Products' Heli-Tran liquid helium cryostat is used to cool a flat copper deposition target to 5 ± 1 K. Neon matrix samples are deposited onto this target just above a Varian TE_{102} X-band microwave cavity whose threaded upper stack has been cut off. This cavity modification reduces the travel distance required to lower the matrix target from the deposition position to its proper position inside the cavity for ESR absorption measurements. The X-band cavity employing 100-kHz modulation is located inside the vacuum chamber. A hydraulic system is used to raise and lower the cryostat (and attached matrix sample) under high-vacuum conditions.

The radical cation was generated by codepositing acetaldehyde vapor and neon under ionizing conditions. The following three independent methods of ionization previously described were employed on numerous depositions during the course of these neon matrix studies: photoionization (PI) at 16.8 eV using an open-tube (9-mm o.d. quartz) neon resonance lamp powered by a microwave generator at 50 W forward and 4 W reflected power;[6] electron bombardment (EB) with 50-eV electrons;[20] and laser multiphoton ionization (MPI) at 355 nm.[21] The neon resonance PI method produced the most intense ESR signals although all three methods produced the extreme preferential orientation characteristics for the acetaldehyde cation in neon matrices described in the next section.

The generation methods produce free or isolated cations with counter negative ions located in separate neon lattice sites separated by an indeterminate number of neon atoms. Since only a small fraction of the neutrals are initially ionized and since many ions are neutralized during the trapping process, it has been estimated that the ratio of neon to trapped cations is $\sim 10^6/1$.[6] The flow rate of matrix neon was 5.0 sccm with an additional flow of 2.5 sccm through the resonance lamp whose open end is located 7 cm from the matrix deposition target. The ratio of neon to acetaldehyde vapor was varied over the range $10^2/1$ to $10^4/1$ with no significant differences in the results except for variations in the ESR signal intensities and for slightly narrower lines in the more dilute matrices. The acetaldehyde vapor did not pass through the discharge source but was deposited into the rapidly condensing neon matrix gas from a separate inlet tube. Typical deposition times were from 30 to 60 min.

(8) Wang, J. T.; Williams, F. *J. Phys. Chem.* **1980**, *84*, 3156.
(9) Grimison, A.; Simpson, G. A. *J. Phys. Chem.* **1968**, *72*, 1176.
(10) Hasegawa, A.; Shiotani, M.; Williams, F. *Faraday Discuss. Chem. Soc.* **1977**, *63*, 157.
(11) Knight, L. B., Jr.; Steadman, J. *J. Chem. Phys.* **1984**, *80*, 1018.
(12) Cochran, E. L.; Adrian, F. J.; Bowers, V. A. *J. Chem. Phys.* **1962**, *36*, 1938. Banks, D.; Gordy, W. *Mol. Phys.* **1973**, *26*, 1555.
(13) Graham, W. R. M.; Weltner, W., Jr. *J. Chem. Phys.* **1976**, *65*, 1516.
(14) Taarit, Y. B.; Symons, M. C. R.; Tench, A. J. *J. Chem. Soc., Faraday Trans.* **1977**, *73*, 1149.
(15) Symons, M. C. R.; Boon, P. J. *Chem. Phys. Lett.* **1982**, *89*, 516.
(16) Snow, L. D.; Williams, F. *Chem. Phys. Lett.* **1983**, *100*, 198.
(17) Symons, M. C. R.; Boon, P. J. *Chem. Phys. Lett.* **1983**, *100*, 203.
(18) Snow, L. D.; Williams, F. *Faraday Discuss. Chem. Soc.* **1984**, *78*, 57.
(19) Boon, P. J.; Symons, M. C. R.; Ushida, K.; Shida, T. *J. Chem. Soc., Perkin Trans. 2* **1984**, 1213.
(20) Knight, L. B., Jr.; Bostick, J. M.; Woodward, J. R.; Steadman, J. *J. Chem. Phys.* **1983**, *78*, 6415.
(21) Knight, L. B., Jr.; Cobranchi, S. T.; Gregory, B. W.; Earl, E. *J. Chem. Phys.*, in press.

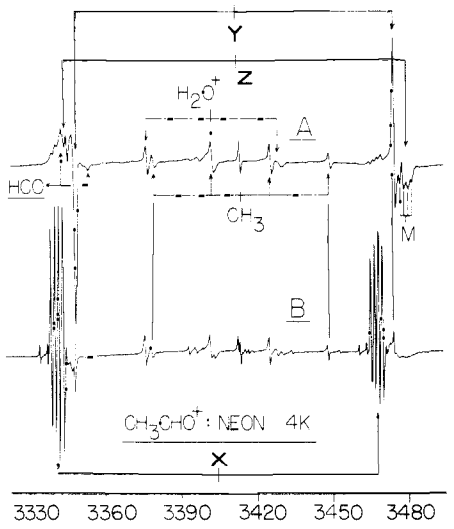

Figure 1. The ESR spectrum of acetaldehyde (CH_3CHO^+) is shown in a neon matrix at 4 K for two different orientations of the trapping surface in the external magnetic field. For spectrum A, the trapping surface is oriented so that a line normal to its surface is perpendicular to the magnetic field ($\theta = 90°$). Similarly, spectrum B was recorded in the $\theta = 0°$ orientation position. See text for assignment of the various angular dependent absorption features. The ESR spectra shown here for neon should be compared with those recorded for CH_3CHO^+ in a Freon ($CFCl_3$) matrix in Figure 2 where the same magnetic field scale is employed.

Attempts to trap the acetaldehyde cation in argon matrices using these generation methods were not successful. This is consistent with previous findings which show that cations having electron affinities much greater than ~10 eV cannot be stabilized in argon whose ionization energy is 15.3 eV,[1] compared to an IE for neon of 21.3 eV.

The intentional introduction of electron-accepting species such as $Cl_2(g)$ and $CCl_4(g)$ did not affect the ESR observations for the acetaldehyde cation radical. Obviously, negative ions are also trapped in the neon matrix, but previous results have shown that sufficient numbers of such counterions can be generated from background impurities; likely candidates include OH^-, N_2^-, and O_2^-,[1] but these are either not radicals or do not have the proper electronic ground state for matrix ESR detection. The direct ESR monitoring of free or isolated cations and anions in the same rare gas matrix has been reported in a recent study of $F_2^-(X^2\Sigma)$,[5] where N_2^+ and H_2O^+ cation radicals were also observed.[1]

Freon Matrices. Solutions containing from 0.5 to 1 mol % of the acetaldehyde in trichlorofluoromethane (Matheson or PCR/SCM Specialty Chemicals) or other Freons were prepared on a vacuum line using degassed solvents stored in portable glass reservoirs fitted with greaseless stopcocks. Acetaldehyde-*1*-d_1 (98.28 atom % D), acetaldehyde-*2,2,2*-d_3 (98 atom % D), and acetaldehyde-d_4 (99 atom % D) from Merck Isotopes and acetaldehyde-h_4 from Aldrich were purified by trap-to-trap distillation immediately before sample preparation. The samples were sealed in 3-mm o.d. synthetic quartz (Spectrosil or Suprasil) tubes and irradiated at 77 K in a cobalt-60 γ source at a dose rate of ca. 0.06 Mrad/h for 4–8 h. A typical dose of 0.3 Mrad corresponds to an energy input of 3×10^3 J kg^{-1}.

ESR measurements were carried out using a Bruker ER 200 D SRC spectrometer equipped with variable-temperature accessories.[16,18] The sample was transferred at 77 K from a movable irradiation Dewar into the Dewar insert mounted in the TE_{102} cavity (ER-4102-ST X-band resonator). Spectra were usually recorded over a wide range of temperature, the upper limit depending on the softening point of the matrix. For $CFCl_3$ the useful range was from 40 to 150 K. The operating microwave frequency was measured with a Systron-Donner 6054B counter, and magnetic field calibration markers were recorded during the scan using either the Walker G-502 or Bruker microprocessor-controlled ER 035 M NMR gaussmeter.

Results

1. CH_3CHO^+ in Neon Matrix. a. Preferential Orientation. The neon ESR results for the acetaldehyde radical cation will be presented first and in more detail than the Freon results since the species has not been previously studied in neon and this is the first example of extreme preferential orientation for a charged radical in a rare gas matrix. Such preferential orientation phenomena have been previously described for several neutral radicals in rare gas matrices[22a] and for fluorocarbon radical anions in hydrocarbon-like matrices.[22b]

The overall ESR spectrum of the acetaldehyde cation radical (CH_3CHO^+) in a neon matrix at 5 ± 1 K is shown in Figure 1 for two different orientations of the flat deposition target in the external magnetic field. The upper trace (A) of Figure 1 is for $\theta = 90°$ where θ is the angle between a line normal to the deposition surface and the applied magnetic field. In the lower trace (B), the matrix surface has been rotated to the $\theta = 0°$ position. The large doublet splitting of ~130 G results from the aldehydic hydrogen in CH_3CHO^+. Resolvable A tensor anisotropy for this H combined with significant g tensor anisotropy produces the overall spectral characteristics shown in Figure 1. The observed line positions and magnetic parameters for CH_3CHO^+ are listed in Table I. Figure 2 shows the ESR spectrum of CH_3CHO^+ trapped in a Freon matrix ($CFCl_3$) which is compared with the neon result in a later section.

Table I. ESR Line Positions and Magnetic Parameters for CH_3CHO^+ in Neon Matrix at 5 ± 1 K[a]

M_1(H)	X[b]	Z[b]	Y[b]
−1/2	3470.6 (2)	3482.8 (6)	3477.7 (2)
+1/2	3344.2 (2)	3349.2 (6)	3351.9 (2)
	g_x = 2.0069 (3)	g_z = 2.0019 (6)	g_y = 2.0026 (3)
	A_x(H) = 126.4 (4) G = 355 (1) MHz	A_z(H) = 133.6 (1.2) G = 374 (3) MHz	A_y(H) = 125.8 G = 353 (1) MHz
	$A_x(CH_3)$ = 1.55 (6) G[c] = 4.3 (2) MHz	$A_z(CH_3)$[d]	$A_y(CH_3)$ < 0.2 G[e] < 0.6 MHz

[a] Microwave frequency is 9574.5 (4) MHz. *A* and *g* values calculated from an exact diagonalization analysis. The *A* values are not the principal components except for A_x. See text. [b] Line positions in gauss. See assignment of molecular axes in Figure 3. [c] Weak lines are also detected which indicate that a small fraction of the CH_3CHO^+ radicals have CH_3 groups which are not undergoing motional averaging; these lines have the same g_x and A_x(H) parameters as those indicated but have two equivalent methyl H's with A = 5.25 (5) G and the other methyl H with A = 2.93 (5) G. This triplet of doublets hyperfine pattern for CH_3 is labeled "TD" in Figure 6. [d] Complex CH_3 structure is observed on this component that seems to have a spacing of 1.8 (2) G. Partial overlap with the intense *Y* component prevents a complete analysis. [e] No resolvable CH_3 structure is seen on this intense *Y* component.

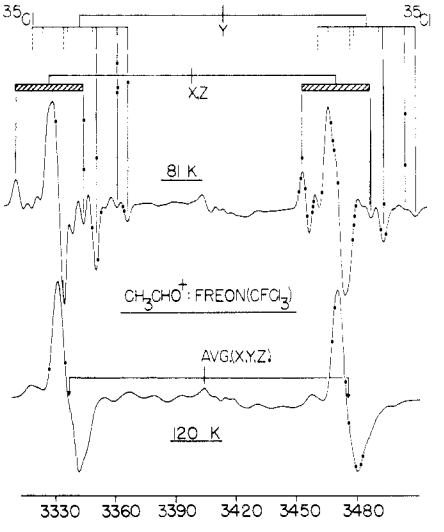

Figure 2. The ESR spectrum of CH_3CHO^+ is shown in a Freon ($CFCl_3$) matrix at two different temperatures. This Freon spectrum should be compared with the neon spectrum for CH_3CHO^+ shown in Figure 1 where the same magnetic field scale has been used. The substructure accompanying the aldehydic hydrogen doublet in the 81 K spectrum is assigned to ^{35}Cl (and ^{37}Cl) hfs which results from a $CH_3CHO^+ - CFCl_3$ complex, only the high-field g_y components being clearly resolved. The stick-diagram reconstruction of this complicated substructure is discussed in the text.

(22) (a) Weltner, W., Jr. *Magnetic Atoms and Molecules*; Van Nostrand-Reinhold: New York, 1983. (b) McNeil, R. I.; Williams, F.; Yim, M. B. *Chem. Phys. Lett.* **1979**, *61*, 293. Morton, J. R.; Preston, K. F.; Wang, J. T.; Williams, F. *Ibid.* **1979**, *64*, 71.

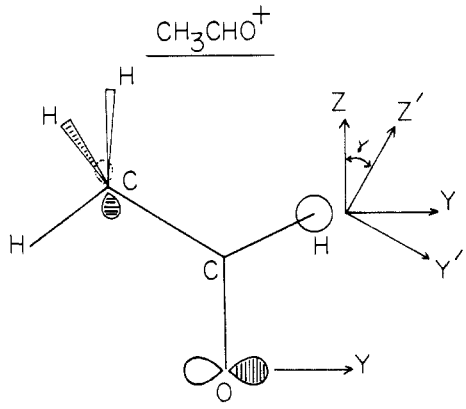

Figure 3. The molecular axes are indicated for CH_3CHO^+ which have been assigned to the **g** and **A** tensor components observed in its neon matrix ESR spectra (see Tables I and II). The X axis is perpendicular to the molecular Y–Z plane. The angle γ is the rotation required to shift the molecular Z and Y axes into the principal **A** tensor directions for the aldehydic hydrogen; see text.

The extreme degree of preferential orientation of CH_3CHO^+ in the neon lattice accounts for the spectral differences that occur when the deposition surface is rotated in the magnetic field. In the $\theta = 0°$ position (Figure 1B), the g_x component dominates while at $\theta = 90°$ (Figure 1A) the intense g_y and weaker g_z components exhibit their maximum intensities. Since the g_z component occurs below g_y at low field and above g_y at high field, the relative phases of these components are reversed and the spectrum in this $\theta = 90°$ position resembles a classic powder-pattern line shape. The ESR analysis and spectral interpretation presented for CH_3CHO^+ in this report are consistent with the preferential orientation arrangement that places the plane defined by the CCHO atoms parallel to the deposition surface. Having this molecular plane (consisting of the heaviest atoms) parallel to the matrix surface is the most common type of preferential orientation observed for radicals in neon matrices.[22] A detailed explanation of the preferential orientation phenomenon in rare gas matrices has not been presented, but it has been suggested that directional heat flow characteristics during the deposition process might be a contributing factor.[23]

The occurrence of preferential orientation for CH_3CHO^+ is indeed fortunate since it produces narrower spectral lines and helps clarify the correlation of the various g and A components. For reasons discussed in the next section, the g_x component is assigned as the direction perpendicular to the molecular plane while g_y and g_z lie in this plane. This would explain why the g_x component dominates at $\theta = 0°$ and why the g_y and g_z lines appear as a powder spectrum at $\theta = 90°$. The g axes are assigned in Figure 3 based on the assumption that the oxygen p orbitals determine the principal directions of the **g** tensor. Since the spin density on oxygen is known to be large and its spin–orbit parameter is considerably greater than that of carbon, this is certainly a reasonable assumption. However, given the small amount of p-orbital spin density on the methyl carbon, it is possible that the in-plane principal **g** tensor directions are rotated a small amount from the y and z directions shown in Figure 3. In the similar H_2CO^+ radical previously investigated by ESR in neon matrices, such an in-plane rotation of axes for the **g** tensor would not occur given the higher symmetry of this cation.

The degree of preferential orientation was observed to vary slightly among the various depositions. This can be seen by comparing the two expanded-scale spectral presentations in Figures 4 and 5 which were recorded for different neon depositions. The results presented in Figure 4 are for a neon matrix deposited approximately 2 K warmer than that for a comparable deposit at 4 K shown in Figure 5. Note that in the warmer deposit, the g_x lines are weak but still detectable at $\theta = 90°$ and the g_z lines

(23) Knight, L. B., Jr.; Easley, W. C.; Weltner, W., Jr. *J. Chem. Phys.* **1971**, *54*, 1610.

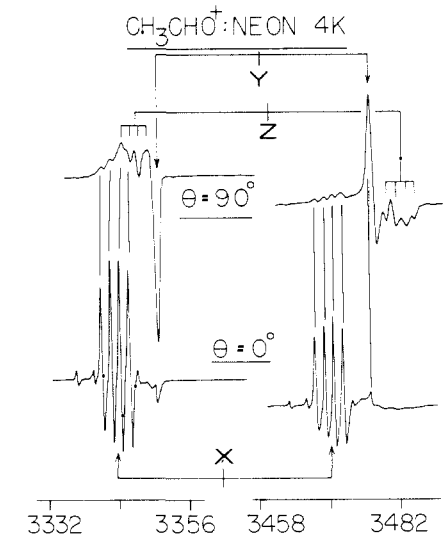

Figure 4. Expanded-scale presentations of the ESR spectra for CH_3CHO^+ are shown which emphasize the preferential orientation characteristics in a neon matrix. θ is the angle between a line normal to the copper trapping surface and the external magnetic field. In this neon sample which was deposited at 6 K, the degree of preferential orientation is not as complete as that shown in Figure 5 which is for a similar deposit at 4 K. Note that in this figure, the g_x lines are still detectable in the $\theta = 90°$ position and the g_y lines are still detectable in the $\theta = 0°$ position; see text.

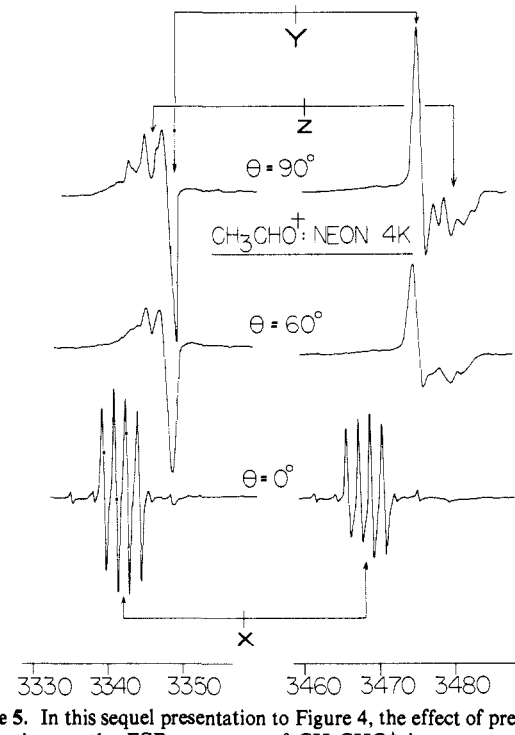

Figure 5. In this sequel presentation to Figure 4, the effect of preferential orientation on the ESR spectrum of CH_3CHO^+ in a neon matrix is shown. θ is the angle between a line normal to the trapping surface and the external magnetic field. This neon sample was deposited at 4 K (2 K colder than that shown in Figure 4) and exhibits a higher degree of preferential orientation. Note that the g_x lines only appear in the $\theta = 0°$ orientation of the trapping surface.

are discernible at $\theta = 0°$. However, for the colder deposit shown in Figure 5, the g_x lines are not detectable at $\theta = 90°$ or $\theta = 60°$ nor the g_z lines at $\theta = 0°$. Hence the degree of preferential orientation is influenced by small temperature changes which presumably affect certain properties of the neon deposition process. Several deposits were also attempted in the 9–11 K range which we have observed as the upper limit where relatively small radicals can be trapped in neon. Under these "warm" deposition conditions, broader ESR absorption envelopes were observed that included

all the features clearly resolved at the lower deposition temperatures. Practically all of the preferential orientation characteristics for CH_3CHO^+ in neon were absent in such warm deposits. Also, the preferential orientation and narrower lines did not appear after cooling these warm deposits to 4 K following deposition. Annealing or warming matrices deposited at the lowest temperatures (4–5 K) to approximately 11 K caused large intensity losses for all signals and caused the g_x lines to shift several gauss upfield and increased A_x by 6 G. Also, the intensity distribution of the g_x lines changed upon severe annealing from the original 1:1:1:1 pattern to a quartet having the intensity ratio of 1:3:3:1; however, the internal spacing in these quartet patterns did not change more than 0.1 G. Presumably the severe annealing creates a larger or less restrictive matrix site which permits the occurrence of nearly free rotation. Such irreversible changes caused by severe annealing have been previously reported.[24]

b. CH_3 Rotation. The intense g_x quartet patterns detected at low and high fields for the two M_I values of the aldehydic H doublet presumably result from acetaldehyde cations whose CH_3 groups are undergoing motional averaging about the in-plane C–C bond direction. The observed 1:1:1:1 intensity ratio for matrices not subjected to severe annealing rather than a 1:3:3:1 pattern is consistent with CH_3 rotating in its lowest state. In this rotational state, the combined nuclear spin wave function must be symmetric; this requires an equal statistical weighting thus producing four equally intense hyperfine lines. This case for the isolated CH_3 radical has been described in detail by other investigators.[25] If these same constraints apply to the nuclear spin statistics in this more complicated case where the CH_3 group is part of a larger radical, then the observed CH_3CHO^+ spectrum is consistent with CH_3 rotation about the C–C axis.

The 1:1:1:1 intensity ratios could also be explained in terms of a dynamical line-broadening effect if the methyl group were to undergo reorientation by a quantum tunneling process.[26-28] However, this would specifically require the reorientation rate at 4 K to coincide closely with the quartet hyperfine splitting (ν) of 4.3 MHz, the critical rate constant for line broadening being $2\pi\nu/2\sqrt{2}$ or 9.6×10^6 s^{-1}.[29] At this coalescence point, the even (E) lines in the 1:1:1:2:1:1:1 pattern for slow reorientation become selectively broadened by exchange effects, leaving only the odd (A) lines at the normal quartet positions.[28] If this were the case here, the spectrum should show a strong temperature dependence. In particular, the E lines would undergo exchange narrowing at higher temperatures to augment the intensities of the inner lines in the quartet and produce a normal 1:3:3:1 distribution. Actually, the intensity ratios of the methyl quartet were observed to change from 1:1:1:1 to 1:3:3:1 in going from 4 to ~11 K. While this result is in accord with the tunneling rotation model, its confirmation would further require the observation of a seven-line pattern below 4 K. Unfortunately, ESR measurements are presently lacking in this region because of experimental constraints.

One alternative to this rotational explanation of the observed intensity distribution for the CH_3 group is for the observed four-line pattern to result from doublet-of-doublet H hyperfine structure which accidentally produces four almost equally spaced lines. This would require all three H's to be inequivalent and have $|A|$ values of 3.1, 1.6, and ~0 G. Three inequivalent H's would not be consistent with theoretical calculations which predict the eclipsed conformation shown in Figure 3 to be the lowest energy state.[30] This eclipsed conformation with two equivalent and one inequivalent hydrogen would yield a triplet-of-doublets pattern as discussed below.

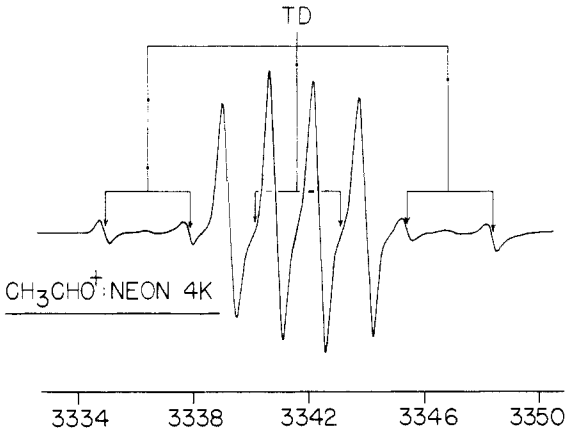

Figure 6. Weaker ESR lines that seem to form a triplet-of-doublets (TD) hydrogen hfs pattern are shown which are centered about the more intense g_x quartet lines. In this highly expanded scale spectrum, the lower field ($M_I = {}^1/_2$) line of the aldehydic hydrogen doublet is shown for CH_3CHO^+. These TD features are tentatively assigned to hydrogen hfs originating from a nonrotating CH_3 group in CH_3CHO^+. In the most stable eclipsed conformation, one hydrogen is in the radical plane while the others are above and below the plane. This arrangement should produce a triplet-of-doublets pattern; see Figure 3.

Therefore, based on these considerations we will consider the g_x lines to be CH_3 quartets whose intensity differs from the normal 1:3:3:1 distribution because of internal rotational effects. However, it should be pointed out that the observed spacings between these unusually narrow lines are not exactly equal. Going from low to high field for both groups, the spacing is 1.61 (3) G between the first and second lines, 1.49 (3) G between the second and third, and 1.61 (3) G between the third and fourth. It is most unusual to be able to measure intervals with this degree of accuracy for matrix isolated radicals. This slight amount of unequal spacing might result from a hindered rotational motion which prevents a complete averaging of the different H environments. There is apparently sufficient rotational motion to alter the nuclear spin statistics but not quite enough to completely average the different environments. While an alternate explanation for this small degree of unequal spacing would be the doublet-of-doublets interpretation discussed above, strong evidence against this argument is that warm neon matrices (~11 K) and those that have been severely annealed (warm to ~12 K and quenched to 4 K) exhibit a g_x quartet pattern that does show an equal spacing of 1.6 (1) G and a 1:3:3:1 intensity distribution.

c. Nonrotating CH_3. For all neon matrices of CH_3CHO^+ deposited at the lowest temperature, weak sets of doublets were detected at $\theta = 0°$ which were centered exactly about the strong g_x quartet pattern at low and high field. These lines can be seen in Figures 1, 4, and 5 and are presented more clearly on the highly expanded scale spectrum of Figure 6 which was recorded for a neon deposit exhibiting a very high degree of preferential orientation as discussed above. It is probable that these outer doublets (see Figure 6) are part of a triplet-of-doublets with the center doublet obscured by the more intense g_x quartet lines. The relative intensity of these TD (triplet-of-doublets) lines never exceeded 12% of the g_x quartet lines. They did not appear on warm deposits and were eliminated by annealing the neon matrix to 10–11 K. The triplet spacing of the TD pattern was 5.25 (5) G with a doublet spacing of 2.93 (5) G. It is suggested in the next section that the TD pattern results from hydrogen hyperfine structure for a nonrotating CH_3 group in CH_3CHO^+. The unique H would be in-plane and eclipsed with the oxygen $2p_y$ orbital while the two equivalent H's giving rise to the triplet hfs would be assigned to the H atoms above and below the molecular plane. See Figure 3.

^{13}C hfs. A very weak doublet hf pattern centered about the low- and high-field g_x quartet lines was observed with the matrix surface in the $\theta = 0°$ position. The internal spacings of these weak

(24) Easley, W. C.; Weltner, W., Jr. *J. Chem. Phys.* **1970**, *52*, 197.
(25) McConnell, H. M. *J. Chem. Phys.* **1958**, *29*, 1422. Morehouse, R. L.; Christiansen, J. J.; Gordy, W. *Ibid.* **1966**, *45*, 1747. Jackel, G. S.; Gordy, W. *Phys. Rev.* **1968**, *176*, 443. Jen, C. K. *Formation and Trapping of Free Radicals*, Bass, A. A., Broida, H. P., Eds.; Academic Press: New York, 1960.
(26) Freed, J. H. *J. Chem. Phys.* **1965**, *43*, 1710.
(27) Davidson, R. B.; Miyagawa, I. *J. Chem. Phys.* **1970**, *52*, 1727.
(28) Geoffroy, M.; Kispert, L. D.; Hwang, J. S. *J. Chem. Phys.* **1979**, *70*, 4238.
(29) Carrington, A.; McLachan, A. D. *Introduction to Magnetic Resonance*; Harper & Row: New York, 1967; Chapter 12, pp 205–208.
(30) Bouma, W. J.; MacLeod, J. K.; Radom, L. *J. Am. Chem. Soc.* **1979**, *101*, 5540.

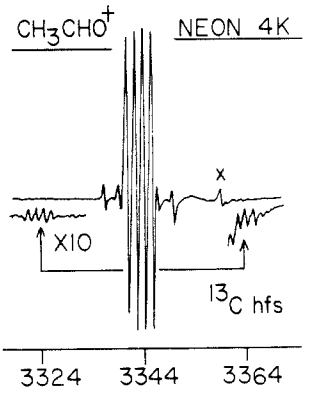

Figure 7. Very weak doublet structure which is centered about the g_x lines is assigned to natural abundance (~1%) ^{13}C hfs in CH_3CHO^+. By analogy with $H_2{}^{13}CO^+$, the observed ^{13}C hfs probably arises from the carbonyl carbon in CH_3CHO^+; see text. The orientation of the trapping surface for this spectrum is $\theta = 0°$.

four-line patterns repeated exactly that observed for the quartet lines. Figure 7 shows that these satellite features are approximately 200 times weaker than the g_x signals. Accordingly, these weak lines with a doublet spacing of 39 (1) G and identical preferential orientation properties to the g_x lines are assigned to the components resulting from natural abundance ^{13}C ($I = {}^1/_2$) nuclear hfs in CH_3CHO^+.

A careful search in the $\theta = 90°$ position for similar ^{13}C structure on the g_z and g_y lines was unsuccessful. Given the broader nature of the g_z and g_y lines, it is not surprising that the ^{13}C hfs could not be detected for these in-plane components. This is unfortunate since the observation of only one **A** tensor component for ^{13}C does not provide sufficient information to describe the spin density in terms of individual isotropic and dipolar contributions. The assignment of the observed ^{13}C hfs in acetaldehyde can be tentatively assigned to the carbonyl carbon based on comparisons with $H_2{}^{13}CO^+$ whose ^{13}C **A** tensor has components of $|A_x| = 44$ G, $|A_y| = 37$ G, and $|A_z| = 35$ G.[11] The signs of these A components are thought to be negative according to ab initio CI calculations for $H_2{}^{13}CO^+$.[31]

2. CH_3CHO^+ in Freon Matrices. The ESR spectra shown in Figure 2 are representative of the low- and high-temperature patterns for CH_3CHO^+ in $CFCl_3$ which are reversible over the useful dynamic range of the matrix. Examples of other ESR spectra recorded for this system between 50 and 158 K have been published.[16,18] The complicated appearance of the low-temperature powder pattern at 81 K reflects the anisotropies of the **g** and both the H and ^{35}Cl hyperfine tensors, as well as the probable noncoincident principal axes of these tensors. While a complete spectral analysis is not possible, some useful structural information can be extracted and shown to be consistent with the results obtained from the neon studies, as discussed below. In contrast, the 120 K spectrum is comparatively unstructured except for the well-defined doublet from the interaction with the aldehydic hydrogen.[11] However, the broad asymmetric lines (10–15 G peak-to-peak line width) indicate that the anisotropy still contributes significantly.

It has already been established by deuterium substitution that the substructure in the low-temperature spectrum does not originate from coupling to the methyl hydrogens or from the anisotropy of the coupling to the aldehydic hydrogen.[16] First, except for an improvement in line resolution, the substructure is unaffected in going from CH_3CHO^+ to CD_3CHO^+ and from CH_3CDO^+ to CD_3CDO^+.[16] Secondly, the wing features on the high-field side of the spectra are virtually identical for CH_3CHO^+ and CH_3CDO^+, and also for CD_3CHO^+ and CD_3CDO^+.[16] The similarity of the features on the high-field side of each substructure is also evident in the 81 K spectrum of Figure 2. It is unlikely that this structure results only from g-anisotropy, and the two most prominent peaks are considered to be the $M_I = -{}^1/_2$ and $-{}^3/_2$ lines of a g_y quartet pattern resulting from a single ^{35}Cl interaction, as indicated in the stick diagram of Figure 2. This analysis is supported by the observed separation between the two outermost ($M_I = -{}^3/_2$) ^{35}Cl and ^{37}Cl peaks which corresponds to ${}^3/_2[(A(^{35}Cl) - A(^{37}Cl)] \simeq 0.25A(^{35}Cl)$, since $A(^{35}Cl)/A(^{37}Cl) = 1.2014$.

From this analysis of the high-field portion of each substructure, the ESR parameters given in Table III were obtained. Clearly, these parameters are associated with the direction along, or close to, the principal axis of the chlorine hyperfine tensor that gives the largest ^{35}Cl coupling. In the molecular axis system of Figure 3, a σ^* complex between the acetaldehyde cation and a chlorine atom from $CFCl_3$ would be expected to involve the overlap of the $2p_y$ orbital on oxygen with a $3p_y$ orbital on the chlorine,[17-19] as shown below, and therefore the y direction should be the principal

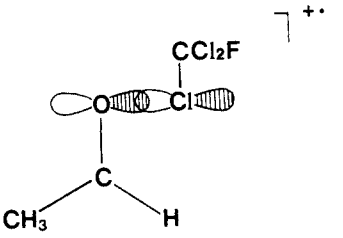

axis corresponding to the largest hyperfine component of the ^{35}Cl hyperfine tensor, provided A_{iso} for Cl is not dominated by negative spin density. We therefore assign the parameters in Table III to the y-tensor components, although these are, of course, not necessarily principal components of the **g** and **A**(^{1}H) tensors.

The above interpretation of the Freon ESR data is consistent with the results of the neon studies in that the g_y components from the two investigations are in reasonably good agreement with each other. Now this agreement would only be expected to occur along the axis of the chlorine p orbital in the complex, since the directions perpendicular to this axis, there should be substantial positive **g** shifts in the complex resulting from the mixing of the SOMO with the other filled chlorine p orbitals. Indeed, this appears to be the case, as discussed below. It is also interesting to note that the $A_y(^1H)$ component is about 15 G larger for the cation–$CFCl_3$ complex than it is for the cation in neon, although we stress that the Freon result is much less precise than the neon value. Despite this reservation and the fact that the other components of the **A**(^{1}H) tensor can only be roughly estimated for the cation–$CFCl_3$ complex, there is little doubt that the average ^{1}H hyperfine coupling for the complexed cation is some 8–9 G larger than the isotropic value for the cation in neon.

The low-field side of the substructures in the 81 K spectrum could not be analyzed by inspection. According to the above structural model of the σ^* complex, the x and z components of the **g** tensor should be larger than the y component, while the ^{35}Cl coupling is expected to be much smaller for these directions. In addition, g_x and g_z may differ significantly, as is the case for the uncomplexed cation in neon. Thus, the x and z features are expected to overlap strongly with each other and with the low-field y line components in this region. This expected spectral congestion accounts for the intense broad absorptions situated slightly downfield from the center of each substructure as indicated by the horizontal bands in the stick diagram of Figure 2. From the positions and widths of these resonances, it is estimated that the average value of g_x and g_z is about 2.008 while the average ^{35}Cl hyperfine splitting in these directions is ca. 6 G.

The 120 K spectrum in Figure 2 shows that much of the substructure associated with the low-temperature spectrum has collapsed. In particular, the line resonances assigned to the outer y features on the high-field side have merged with the strong absorptions attributed mainly to the x and z features. Nevertheless, the total absorption envelope for each of these doublet features still extends for 30–40 G and some unresolved structure is still apparent, as indicated by the prominent hmps displayed on the low-field side of the main absorption lines. The average ESR parameters for this high-temperature doublet (Table III) were calculated from the "crossover" points of the broad lines, which also correspond reasonably well to the centers of gravity of the features. While these parameters ($g_{av} = 2.005 - 2.006$,

Table II. Comparison of the Magnetic Parameters (MHz) for H_2CO^+ and CH_3CHO^+ in Neon Matrices at 4 K

	H_2CO^+	CH_3CHO^+
g_x[a]	2.0069 (2)	2.0069 (3)
g_y	2.0015 (2)	2.0026 (3)
g_z	2.0025 (3)	2.0019 (6)
g_{iso}	2.0036 (3)	2.0038 (4)
A_x[b]	363.4 (6)	355 (1)
A_y	376.7 (6)	353 (1)
A_z	376.3 (6)	374 (3)
A_{iso}	372.1 (6)	361 (2)
A_x(dip)[c]	−9 (1); (−10)[d]	−6 (3)
A_y(dip)	5 (1); (3.4)	−8 (3)
A_z(dip)	4 (1); (7.0)	13 (5)

[a] g and A tensors are assigned to the molecular axes given in Figure 3. [b] All A values are for the aldehydic hydrogen and are not the principal components except for A_x. See text. [c] $A_x(\text{dip}) = (A_x - A_{iso})$, etc. [d] For H_2CO^+ the calculated dipolar components in parentheses are in the molecular axis system which are not necessarily the principal components. See ref 11 and 31.

$A_{av}(^1H)$ = 136–137 G) clearly differ from the isotropic values for the cation in neon (Table II), they correspond closely to the values expected from the averaging of the anisotropic parameters for the low-temperature spectrum. In other words, the higher average g factor and ^1H hyperfine coupling associated with the complex form of the cation at low temperature are both retained at the higher temperature. The major change, which is the collapse in the substructure resulting from the chlorine interaction, is therefore also taken to be an averaging effect, so we postulate that the A_x and A_z components (ca. 6 G) of the ^{35}Cl hyperfine tensor are negative, whereas the A_y component (ca. 17 G) is positive. Consequently, the apparent loss of the chlorine coupling is simply attributable to the spectrum becoming less anisotropic in the high-temperatre regime, a rather common occurrence in solid-state studies.

Studies of the acetaldehyde radical cation were also carried out in the CF_3CCl_3 matrix. In this case the substructure of the doublet spectrum at 80 K was even broader (ca. 80 G) and less well-resolved than that observed in the $CFCl_3$ matrix. Again the substructure narrowed considerably on warming the matrix to 130 K, and this change was also reversible.

Discussion

Comparison of the Neon Results for H_2CO^+ and CH_3CHO^+. The large hydrogen hfs observed in CH_3CHO^+ is comparable to that of similar radicals such as H_2CN (A = 87 G),[12] H_2BO (A = 133 G),[13] and H_2CO^+ (A_{iso} = 133 G).[11] Only in the H_2CO^+ and $H_2{}^{13}CO^+$ cases has a detailed analysis of the **g** and **A** tensors been possible since this radical ion does not undergo motional averaging in neon and its ESR spectrum in neon matrices was fully resolved. For H_2CO^+ there has also been ab initio CI theoretical calculations of the ^{13}C and H magnetic parameters which indicate extreme sensitivity to the C–O bond length employed.[31]

ESR studies for H_2CO^+ have only been reported in neon matrices,[11] and attempts to trap it in other media such as Freons have not been successful.[2,32] It was somewhat surprising in the neon H_2CO^+ study that the preferred assignment of g values to specific directions in the radical indicated that the direction of greatest g shift occurred perpendicular to the molecular plane. Previous to this H_2CO^+ study, it was usually assumed that the greatest g shift would have occurred in-plane along the C–O bond direction. In addition to other considerations, comparison of the observed and calculated (CI) ^{13}C **A** tensor components was used to assign the g axes in the $H_2{}^{13}CO^+$ radical.[11] The **g**-tensor assignments made for H_2CO^+ which did not exhibit preferential orientation in neon are consistent with those obtained in this neon investigation of CH_3CHO^+. The methyl rotation effects, preferential orientation, reduced symmetry, and the rather unusual responses to small temperature changes cause the ESR analysis of CH_3CHO^+ to be considerably more complex than the interpretation of the H_2CO^+ ESR spectrum. A detailed comparison of the ESR results for these two similar cation radicals is presented below.

The magnetic parameters for CH_3CHO^+ and H_2CO^+ in neon matrices at 4 K are compared in Table II. The observation of only one **g** tensor component in the $\theta = 0°$ position of the trapping surface for CH_3CHO^+ offers independent evidence that this direction should be assigned perpendicular to the radical plane. This is also the direction of the greatest g shift and is identical within the stated experimental uncertainty limits with the g_x value of 2.0069 (3) observed for H_2CO^+. The in-plane g_y and g_z components for CH_3CHO^+ show no deviation from g_e within the indicated uncertainty limits which are somewhat larger than those obtained for H_2CO^+. Figure 3 gives the assignment of axes used throughout this discussion for the CH_3CHO^+ and H_2CO^+ cases. The dipolar parameters of Table II are defined as $A_x(\text{dip}) = A_x - A_{iso}$ and similarly for the other axes.

Since the unpaired electron in both radicals has significant oxygen $2p_y$ character and since the spin–orbit parameter for oxygen is 5.4 times larger than that of carbon, the observation of similar **g** tensors is expected. The nature of the excited electronic state involved in the dominant spin–orbit coupling to the ground state and the direction of the large g_x shift from g_e have been discussed in detail in the H_2CO^+ report.[11] Whether the principal directions of the **g** tensor for CH_3CHO^+ differ slightly from the in-plane y and z axes shown in Figure 3 cannot be determined from these measurements; small deviation may occur on account of carbon p orbital spin density on the CH_3 group which is predicted by theoretical calculations.[30]

The A_{iso} value for the aldehydic H in CH_3CHO^+ is only 3% less than that for H_2CO^+. Close agreement also exists between the small negative values of A_x(dip) for both radicals. An ab initio CI calculation of A_x(dip) for H_2CO^+ shows close agreement with experiment (see Table II). The dipolar parameter should be negative in the X direction (perpendicular to the molecular plane) since the angular factor of the dipolar operator ($3\cos^2\alpha - 1$) has its maximum negative value of −1 for $\alpha = 90°$, where α is the angle between the applied magnetic field direction at the H nucleus and the position of the unpaired electron. Since the odd electron occupies predominantly in-plane orbitals, the effective value of α along X will be close to 90°.

The in-plane A_y and A_z dipolar components for H are more difficult to interpret, but they provide the most direct information concerning electronic structure differences which occur when H is replaced by CH_3 in the CH_3CHO^+ radical. Such small anisotropic parameters cannot usually be resolved in condensed-phase studies; however, in this case the lines are unusually narrow and the preferential orientation of CH_3CHO^+ in neon makes a more detailed assignment possible. For example, the line width of the g_x lines is only 0.2 G. In H_2CO^+, the A_y and A_z dipolar values were equivalent within the uncertainty limits, both being small and positive (~5 MHz). An attempt to account for the observed changes that occur in these parameters in CH_3CHO^+ will be made in the following highly qualitative manner. As shown by the data in Table II, the dipolar component assigned to the Z direction increases from 4 (1) to +13 (5) MHz going from H_2CO^+ to CH_3CHO^+, respectively. Several factors have to be considered to account for this increase. Let us assume that the spin density on the carbonyl carbon and that in the O $2p_y$ orbital are similar for both radicals. Certainly this latter assumption is reasonable given the identical g_x values. Changes at the carbonyl carbon probably occur but these will be considered later. Along the Z direction, the O $2p_y$ spin density should make a small positive dipolar contribution at the aldehydic H whose magnitude should be similar in both radicals. Spin density in the 1s orbital on the "other" H in H_2CO^+ would make a negative contribution of about 3 MHz along Z since $\alpha \approx 90°$. This calculation is based on distances listed in the H_2CO^+ report, the measured spin density, and simple dipolar expressions given by Gordy.[35] Replacement of the 1s spin density on this "other" H with a CH_3 group where

(31) Davidson, E. R.; Feller, D. *J. Chem. Phys.* **1984**, *80*, 1026.
(32) Symons, M. C. R.; Chen, T.; Glidewell, C. *J. Chem. Soc., Chem. Commun.* **1983**, 326.

Table III. Magnetic Parameters for Acetaldehyde Radical Cations in Freon Matrices

radical cation	matrix	T/K	g[a]	hyperfine couplings[a] (G)	
CH_3CHO^+	$CFCl_3$	81	2.002 (1) (g_y)	141 (A_y(H))	16.0 ($A_y(^{35}Cl)$)
		86			16.1 ($A_y(^{35}Cl)$)
		120	2.006 (1) (g_{av})	137 (A_{av}(H))	
CD_3CHO^+	$CFCl_3$	50			18.4 ($A_y(^{35}Cl)$)
		77			17.3 ($A_y(^{35}Cl)$)
CD_3CDO^+	$CFCl_3$	150	2.006 (1) (g_{av})	20.8 (A_{av}(D))	
CH_3CHO^+	CF_3CCl_3	130	2.005 (1) (g_{av})	136 (A_{av}(H))	

[a] The values of g and A quoted at 120 K and above are averages deduced from the crossover line positions of the broad doublet spectrum (see text and Figure 2). [b] Couplings are to the aldehydic hydrogen (or deuterium) of the acetaldehyde and to one chlorine in $CFCl_3$.

spin density would occur predominantly in a C 2p orbital oriented approximately as shown in Figure 3 would make a near-zero dipolar contribution along Z at the aldehydic H in CH_3CHO^+. Hence a decrease or loss of this negative effect would make the observed A_z(dip) parameter increase in CH_3CHO^+. The C 2p spin density would probably make less of a negative contribution for three independent reasons: (a) The greater C–C distance (1.5 Å) relative to C–H (1.1 Å) would reduce any contribution given the r^{-3} dependence. (b) The axis of the C 2p orbital is nearly parallel to the Z direction. For this relative orientation at smaller distances, experiment and theory show that the dipolar contribution is virtually zero.[35] (c) There could be less spin density on the methyl carbon relative to an H atom at that position. Isotopically labeled $^{13}CH_3CHO^+$ studies would be required to determine if such a reduction occurred.

The observed decrease in A_y(dip) at the aldehydic H in CH_3CHO^+ is consistent with the above factors which seem to account for an increase in A_z(dip). Spin density in O $2p_y$ would most probably make a negative contribution in the Y direction at the aldehydic H since the oxygen electronic distribution closest to H lies at an angle of approximately 80°. In H_2CO^+, this negative contribution from oxygen would be reduced by a positive contribution along Y from the 1s spin density on the "other" H since α would lie close to 0°. This parallel positive contribution can be estimated at ~6 MHz based on procedures already described. When CH_3 replaces H, this positive contribution would be decreased because of the distance factor and possibly less spin density on the methyl carbon. The angular contribution in this direction is more difficult to estimate.

The above qualitative considerations account at least for the direction of change observed for the in-plane components of the dipolar tensor for the aldehydic hydrogen going from H_2CO^+ to CH_3CHO^+. Negative spin density in the $2p_x$ orbital of the carbonyl carbon makes the following dipolar contributions at H: nearly zero along the principle X direction, positive effect in-plane perpendicular to C–H bond, and negative effect in-plane along C–H bond direction. The in-plane perpendicular direction to the C–H bond lies about 28° off the Z axis of Figure 3. Hence $2p_x$ negative spin density on the carbonyl carbon would contribute in a positive manner to A_z(dip). Similarly, such negative spin density would make a negative contribution to A_y(dip). In the previous $H_2{}^{13}CO^+$ study, it was found that a negative spin density of ~0.1 did occur in the carbon $2p_x$ orbital. We estimate that even such a small amount of negative spin density would contribute approximately −3 MHz to A_y(dip) and +3 MHz to A_z(dip). Therefore, a small increase in the carbonyl carbon $2p_x$ negative spin density in CH_3CHO^+ relative to H_2CO^+ would also be consistent with the observed changes in the dipolar tensor of the aldehydic H.

The small shift in the A_x(dip) parameter from −9 (1) to −6 (3) MHz going from H_2CO^+ to CH_3CHO^+ can also be accounted for by the same effects which seem to explain the observed changes for the in-plane dipolar components of H. Spin density in $2p_x$ of the carbonyl carbon makes essentially no contribution at H; hence a change in this orbital would not affect A_x(dip). The negative contribution from the O $2p_y$ would be essentially the same for both radicals for reasons already stated. Spin density on the methyl carbon would probably not make as large a negative contribution given the greater distance relative to an H atom at that position. Therefore, the small change observed in A_x(dip) could result from the same or less spin density on the methyl carbon.

Obviously, a more quantitative calculation is needed but these considerations seem to account for the observed differences between the H_2CO^+ and CH_3CHO^+ cation radicals. A detailed comparison at the ab initio level of theory for these rather delicate molecular properties should prove to be a challenging and worthwhile endeavor.

The A_y and A_z tensor components observed for the aldehydic H in CH_3CHO^+ are in the principal coordinate system of the molecular **g** tensor and are not the principal values of the hydrogen **A** tensor. However, the observed A_x splitting perpendicular to the molecular plane is a principal component since this direction coincides with the g_x direction. The in-plane principal values of the hydrogen **A** tensor cannot be observed directly in these experiments since random orientation occurs in the molecular planes parallel to the trapping surface. However, the in-plane anisotropy is small and the principal components will not differ substantially from those observed in the **g** tensor axis system. With reference to the detailed equations presented in the H_2CO^+ report,[11] the experimental A parameters actually measured or determined in the **g** tensor coordinate system are $(A_{yy}^2 + A_{yz}^2)^{1/2}$ and $(A_{zz}^2 + A_{yz}^2)^{1/2}$. Rotation of these in-plane Y and Z axes by some angle γ will cause Y' and Z' to lie along the principal axis directions of the hydrogen **A** tensor yielding principal components A'_y and A'_z (see Figure 3). Using the apparent or measured A parameters, a rotation of 22° corresponds to an A_{yz} value of 10 MHz. This amount of rotation produces principal component A'_y and A'_z values of 349 and 378 MHz compared to the apparent hfs of 353 and 374 MHz, respectively. The A_{iso} parameter is not affected by this rotation, but the anisotropy in the YZ plane increases to 17 MHz in the Z' direction compared to the nonprincipal value of 13 MHz in the Z direction listed in Table II. Similarly, the −8 MHz dipolar component along Y changes to −12 MHz along the principal Y' direction. Hence, the hydrogen **A** tensor anisotropy is greater than that actually measured in the **g** tensor coordinate system. This is a general characteristic of powder ESR spectra for radicals with noncoincident **g** and **A** tensors, and its effects have been previously discussed by other investigators.[33]

Motional Effects. The ESR observations provide evidence that CH_3CHO^+ exists in two different states in the neon lattice. It appears that approximately 90% of the radicals are trapped in a neon site that permits some type of rotational averaging about the C–C bond while the remainder of the CH_3CHO^+ ions occupy a site that does not allow such motional behavior. An alternate description would be that all radicals occupy essentially the same type of site, but an equilibrium exists between those that undergo CH_3 rotation and those that do not. The limited temperature range available in neon matrices makes a choice between these two different possibilities difficult based on experimental results. The intense g_x quartet lines with a spacing of approximated 1.55 (5) G and a 1:1:1:1 intensity distribution are assigned to CH_3CHO^+ radicals whose CH_3 group is undergoing motional averaging. Both internal barriers and trapping site restrictions could be hindering the rotational motion, but on the ESR time scale the differences that would exist in the hydrogen environments for a static molecule seem to be averaged. The remainder of the radical is thought to remain fairly stationary during the methyl

(33) Golding, R. M.; Tennant, W. C. *Mol. Phys.* **1973**, *25*, 1163.

group rotation. The rotation of an entire molecule the size of CH_3CHO^+ has not been observed in neon matrices presumably because of the small trapping sites available in the lattice. The CH_3 radical is routinely trapped in neon matrices as a background impurity and its presence is indicated in Figure 1. At low microwave power levels in neon, the CH_3 quartet approaches closely the 1:1:1:1 intensity distribution predicted for its lowest rotational state by theoretical considerations (previously discussed) and observed by others in the heavier rare gases.[25]

This type of rotation for the CH_3 group in CH_3CHO^+ would cause its H hfs to appear axially symmetric if the radical could be observed parallel and perpendicular to the C–C bond direction. However, since the C–C direction is not coincident with a principal axis of the molecular **g** tensor, the spectrum is more complicated when the radical is observed in the Y–Z plane, i.e., the $\theta = 90°$ position of the trapping surface. The X axis, perpendicular to the molecular plane and the C–C direction, is a principal g axis, and the methyl H hfs in this direction produces nearly symmetrical and extremely narrow lines. This X direction can be viewed exclusively when the trapping surface is in the $\theta = 0°$ position since CH_3CHO^+ is preferentially oriented in the neon lattice. Anisotropy in the CH_3 hfs is clearly evident in the Y–Z plane as shown by the upper spectrum ($\theta = 90°$) of Figure 4. The broader and weaker Z lines do show resolvable methyl H hfs whose spacings are within 0.2 G to that of the g_x quartet lines. The intense Y lines do not show such resolvable structure. Hence to a reasonable approximation, the CH_3 hfs in CH_3CHO^+ does exhibit axial symmetry as would be expected for a rotating methyl group.

The occurrence of methyl group rotation in CH_3CHO^+ at 4 K is somewhat surprising since the rotational barrier has been calculated to be 0.79 kcal mol^{-1}.[30] However, there are examples of almost free internal rotation at 4 K such as the $CH_3C(COOH)_2$ radical in the methyl malonic acid crystal.[34] Restrictions to internal rotations in crystal media have also been associated with intermolecular hydrogen-bonding type interactions which would not be involved for the isolated acetaldehyde cation in neon matrices. Even though the thermal energies available are considerably less than the calculated barrier to internal rotation, a tunneling mechanism could be involved, as discussed earlier.[35] Whether the rotational motion is hindered or relatively free cannot be determined by these matrix studies, and unfortunately it cannot be studied over a wide temperature range in neon since above 10 K molecular diffusion occurs. The lowest energy conformer of CH_3CHO^+ has a methyl H eclipsed with the oxygen $2p_y$ orbital as shown in Figure 3. The spectral evidence obtained on the various neon depositions and the observed temperature dependence seem to indicate that this triplet-of-doublet hfs which has the same g value as the g_x quartet lines should be assigned to CH_3CHO^+ radicals in this predicted eclipsed conformation (see Figure 6). This conformation does have one unique methyl H and two equivalent H's which would yield a triplet-of-doublets pattern. Unfortunately, the central doublet of the triplet is obscured by the more intense lines of the rotating CH_3 group; thus this triplet-of-doublets assignment cannot be completely verified. Since these features were observed in a reproducible manner on all the numerous independent experiments, it is difficult to propose an alternative explanation. However, a problem with this assignment is that the weighted average of the A values ($|A| = 5.25$ (5) G for two H's and $|A| = 2.93$ (5) G for the unique H), regardless of which signs are chosen for this triplet-of-doublet pattern, does not yield the quartet A value of 1.55 (6) G within the uncertainty limits. Of course, this would only be expected if complete rotational averaging were occurring, and evidence previously cited indicates that the averaging is most probably incomplete.

Comparison of CH_3CHO^+ Results in Neon and Freon Matrices. Although the low-temperature ESR spectra of the acetaldehyde cation in these two matrices have a very different appearance, it can be argued that most of this difference is attributable to the formation of a weak σ^* complex between the cation and the $CFCl_3$ or other Freon solvent employed. In terms of experimental practice, however, the excellent resolution of the spectrum in neon stands in sharp contrast to the broad anisotropic lines in Freon. As a result, detailed information has been extracted from the neon study to characterize the **g** and **A** tensors. In turn, this information helps to resolve conflicts in the interpretation of the Freon results. Thus, a singular achievement of the studies in neon is the resolution of the 1.6-G coupling to the methyl hydrogens. At the same time, this finding has important ramifications for the Freon studies since it provides independent evidence that the extensive substructure observed in $CFCl_3$ does not originate from coupling to the methyl hydrogens,[16] as was first supposed.[15]

Taken together, the results of our combined studies also clarify the structure of the halogen complex which is, in fact, responsible for this substructure. Using the **g**-tensor data provided by the analysis of the spectrum in neon (Table II), it is clear that the largest ^{35}Cl hyperfine coupling observed in the spectrum of the complex is along the Y direction of the cation shown in Figure 3, since this is also found to be the direction corresponding to one of the lower g values in the YZ plane. This finding is consistent with the formation of the proposed σ^* structure.

The availability of the ESR parameters for the uncomplexed cation also helps to shed some light on the controversy regarding the interpretation of the reversible change that the ESR spectrum of the complexed cation undergoes with temperature in the Freon matrix (Figure 2). Symons[36] has argued strongly that the loss of substructure in the spectrum results from a reversible dissociation of the σ^* complex, whereas Snow and Williams[16,18,37] have attributed the spectral change to a partial motional averaging of the chlorine hyperfine anisotropy in the complex. Comparison of the isotropic values of $A(^1H)$ and g calculated from the tensor data in neon (Tables I and II) with the average (x, y, z) parameters derived directly from the 120 K spectrum in $CFCl_3$ show appreciable differences (Table III), suggesting that the cation structure at 120 K in Freon is not the same as that in neon. This conclusion is consistent with the general appearance of the 120 K spectrum under careful examination, the breadth of the lines and the associated low-field humps indicating that the halogen hyperfine interaction is still present, but that the anisotropic coupling is reduced by motional averaging. Also, the fact that the overall width of the anisotropic features resulting from the chlorine interaction gradually decreases with increasing temperature (Table III) supports the latter view.[16,18,37]

Another approach to this question of σ^* complex dissociability in Freon is to make a direct comparison between the 4 K spectrum in neon (Figure 1) and the 120 K spectrum in Freon (Figure 2). If both of these doublet spectra are of the uncomplexed radical cation, some relationship would be expected to exist between the doublet line shapes and/or line widths in the less well-resolved Freon spectrum and the envelopes reconstructed from the resolved x, y, and z features in neon. In the latter case, it is clear that the widths of the two absorption envelopes are quite dissimilar, the low-field and high-field features extending for 10.4 and 17.3 G, respectively, in Figure 1. On the other hand, the two broad lines in the Freon spectrum of Figure 2 at 120 K have about the same total width and are virtually superimposable on each other. This difference between the neon and Freon results therefore does not support the idea[36] that the radical cation σ^* complex in Freon is dissociated at 120 K.

It is also difficult to reconcile this dissociation hypothesis with the results of a recent comparative study in SF_6.[38] The ESR spectra of CH_3CHO^+ and CD_3CHO^+ in this matrix showed no evidence for a solvent interaction at low temperatures, each spectrum consisting of a simple doublet. Accurate isotropic parameters for these uncomplexed cations were obtained from the spectra recorded above 94 K in the SF_6 rotator phase, the average

(34) Heller, C. *J. Chem. Phys.* **1962**, *36*, 175.
(35) Gordy, W. *Theory and Application of Electron Spin Resonance*; Wiley: New York, 1980.
(36) Symons, M. C. R. *Faraday Discuss. Chem. Soc.* **1984**, *78*, 96.
(37) Williams, F. *Faraday Discuss. Chem. Soc.* **1984**, *78*, 105.
(38) Qui, X.-Z.; Guo, Q.-X.; Williams, F., unpublished work.

values being $A_{iso}(^1H)$ = 127.2 G and g_{iso} = 2.0042. Since these results are very similar to those calculated from the neon data, namely, $A_{iso}(^1H)$ = 128.6 G and g_{iso} = 2.0038, it is reasonable to conclude that these parameters are characteristic of the uncomplexed cation irrespective of the nature of the matrix. Consequently, the significantly different parameters observed for the cation above 120 K in the $CFCl_3$ matrix (Table III) now become anomalous for a dissociated cation. On the other hand, these 120 K parameters are just what would be expected if the complex persists and the loss of fine structure results simply from a motional averaging of the ^{35}Cl hyperfine tensor components.

Except for a recent investigation of the cubane radical cation ($C_8H_8^+$),[39] the acetaldehyde ion is the largest cation studied to date by the neon matrix ESR method. Given the high resolution that can be achieved in neon and the chance of preferential orientation, it seems that much larger molecular ions could be analyzed in detail in this host material which has been used primarily for diatomic and triatomic radical ions.[1] A wide range of ion generation and deposition techniques allows neon to be used for nonvolatile inorganic ions[40] including the trapping of ion intermediates produced under reactive laser sputtering[21] and other high-energy conditions.[41] The use of the neon ESR matrix technique for studying ion products formed in ion–neutral reactions has also been demonstrated for the following reactions which are important in stratospheric chemistry: $CO + CO^+ \rightarrow C_2O_2^+$,[42] $N_2 + N_2^+ \rightarrow N_4^+$,[43] $N_2 + CO^+ \rightarrow N_2CO^+$,[1] and $O_2 + O_2^+ \rightarrow O_4^+$.[44]

Acknowledgment. The neon matrix ESR experiments were conducted at Furman University with support from the National Science Foundation (CHE-8508085), the General Electric Foundation, the Amoco Foundation, and Research Corporation. A new ESR spectrometer was made possible by a chemistry equipment grant to Furman University from the Pew Memorial Trust. The Freon experiments conducted at the University of Tennessee were supported by the Division of Chemical Sciences, Office of Basic Energy Sciences, U.S. Department of Energy.

Registry No. CH_3CHO^+, 36505-03-0; Ne, 7440-01-9; $CFCl_3$, 75-69-4.

(39) Knight, L. B., Jr.; Arrington, C. A.; Gregory, B. W.; Cobranchi, S. T.; Liang, S.; Paquette, L. *J. Am. Chem. Soc.* **1987**, *109*, 5521.
(40) Knight, L. B., Jr.; Ligon, A.; Woodward, J. R.; Feller, D.; Davidson, E. R. *J. Am. Chem. Soc.* **1985**, *107*, 2857.
(41) Knight, L. B., Jr.; Miller, P. K.; Steadman, J. *J. Chem. Phys.* **1984**, *80*, 4587.
(42) Knight, L. B., Jr.; Steadman, J.; Miller, P. K.; Bowman, D. E.; Davidson, E. R.; Feller, D. *J. Chem. Phys.* **1984**, *80*, 4593.
(43) Knight, L. B., Jr.; Johannessen, K. D.; Cobranchi, D. C.; Earl, E.; Davidson, E. R.; Feller, D. *J. Chem. Phys.* **1987**, *87*, 885.
(44) Knight, L. B., Jr.; Davison, E. R., to be published.

High-Resolution Solid-State ^{13}C NMR Spectra of Porphine and 5,10,15,20-Tetraalkylporphyrins: Implications for the N–H Tautomerization Process

Lucio Frydman,[†] Alejandro C. Olivieri,[†] Luis E. Diaz,[†] Benjamin Frydman,*[†] Frederick G. Morin,[‡] Charles L. Mayne,[‡] David M. Grant,[‡] and Alan D. Adler[§]

Contribution from the Facultad de Farmacia y Bioquimica, Universidad de Buenos Aires, Junin 956, Buenos Aires 1113, Argentina, Department of Chemistry, University of Utah, Salt Lake City, Utah 84112, and Chemistry Department, Western Connecticut State University, Danbury, Connecticut 06810. *Received March 30, 1987*

Abstract: The solid-state high-resolution ^{13}C nuclear magnetic resonance spectra of porphine and of 5,10,15,20-tetraalkylporphyrins were recorded with use of the CP/MAS technique. The solution kinetics of the hydrogen migration between the two tautomers of porphine, *meso*-tetrapropyl- and *meso*-tetrahexylporphyrins, were also studied, and the activation parameters were found to be similar to those reported in the literature for tetraarylporphyrins. Porphine showed the same dynamical behavior in the solid state as in solution, while in the solid state the tetraalkylporphyrins showed doubling of the pyrrole carbon resonances at room temperature. The results obtained with the tetraalkylporphyrins can be explained assuming either a proton-transfer reaction slow on the NMR time scale or a fast exchange between two unequally populated tautomers. Three hypotheses are discussed with regard to the kinetic solid-state effects involved: (a) a quenching of the tunneling contribution to the proton-migration process; (b) a fixed geometry adopted by the four nitrogen atoms in the crystal that controls the migration; (c) a coupling between the proton-exchange process and the deformation of the porphyrin skeleton, the latter being hindered by neighboring molecules.

Porphyrins and porphyrin derivatives have attracted considerable attention due to the biological relevance of these naturally occurring compounds. In addition, these molecules have an intrinsic significance in chemistry because of their unique electronic structure, the large number of synthetic structures available for study, and the many phenomena that they exhibit.[1-3]

Free-base porphyrins have two protons in the inner part of the skeleton. Early information about the localization of these hydrogens in the framework of the four nitrogen atoms came from X-ray crystallographic studies.[4-6] However, most of the experimental observations of interest regarding the migration of these two hydrogens among the four nitrogens have been obtained from solution NMR spectroscopy.[7-12]

[†] Universidad de Buenos Aires.
[‡] University of Utah.
[§] Western Connecticut State University.

(1) Adler, A., Ed. *Ann. N.Y. Acad. Sci.* **1973**, *206*.
(2) Smith, K., Ed. *Porphyrins and Metalloporphyrins*; Elsevier: Amsterdam, 1975.
(3) Dolphin, D., Ed. *The Porphyrins*; Academic: New York, 1979.
(4) Silvers, S. J.; Tulinsky, A. *J. Am. Chem. Soc.* **1967**, *89*, 3331.
(5) Hamor, M. J.; Hamor, T. A.; Hoard, J. L. *J. Am. Chem. Soc.* **1964**, *86*, 2305.
(6) Webb, L. E.; Fleischer, E. B. *J. Chem. Phys.* **1965**, *43*, 3100.
(7) Storm, C. B.; Teklu, Y. *J. Am. Chem. Soc.* **1972**, *94*, 1745.

0002-7863/88/1510-0336$01.50/0